

Inverse Roughening Transition in the Staggered Body-Centered Solid-on-Solid Model

Erik Luijten* and Henk van Beijeren

Institute for Theoretical Physics, Utrecht University, P.O. Box 80006, 3508 TA Utrecht, The Netherlands

Henk W. J. Blöte

Faculty of Applied Physics, Delft University of Technology, P.O. Box 5046, 2600 GA Delft, The Netherlands

(Received 20 April 1994)

The F model and inverse F model in a staggered electric field are examined by using transfer matrices and finite-size scaling. It is shown that such a field induces a Kosterlitz-Thouless transition in the inverse F model, corresponding to an "inverse" roughening transition in the body-centered solid-on-solid representation: a crystal facet appears *above* a certain temperature. It disappears again in the limit of infinite temperature. We find the location of this phase transition as a function of staggered field and for a specific choice of this field we estimate the facet size as a function of temperature.

PACS numbers: 68.35.Bs, 68.35.Rh, 64.60.Cn, 64.60.Fr

A well-known class of two-dimensional lattice models is formed by the six-vertex or ice-type models [1]. By assigning different energies to the six vertices which occur in these models (see Fig. 1), both ferroelectric and antiferroelectric systems can be modeled. If the vertex weights are chosen uniformly throughout the lattice these models can be solved exactly and shown to exhibit phase transitions of various kinds [2–5]. By assigning height differences to the vertices, one obtains body-centered solid-on-solid (BCSOS) models, a class of solid-on-solid surface models [6], which can be used to study crystal surfaces. A well-known six-vertex model is the F model [7], which has been solved exactly by Lieb [2] (this solution was generalized by others [3,4]) and which displays a phase transition of Kosterlitz-Thouless nature at a certain temperature T_R , with $k_B T_R = e/\ln 2$, where e is the vertex energy introduced in Fig. 1. In the BCSOS model this phase transition corresponds to a roughening transition. This transition takes place because the occurrence of vertices 1 to 4, and thus of height differences between next-nearest neighbors, increases.

The ground state of the F model is antiferroelectric, consisting of a checkerboard pattern of vertices 5 and 6. The twofold degeneracy of this ground state can be removed by a staggered electric field, i.e., a field which alternates in direction on neighboring arrows and thus discerns the two sublattices in the model. This field forces the F model above T_R from an algebraic phase into an ordered state [8]. Unfortunately, it is not pos-

sible to solve the model in the presence of such a field, except for $T = 2T_R$ [9], so that the behavior of the F model in a staggered field is not well known. The importance of this unsolved problem was emphasized by, e.g., Lieb and Wu [1] and Baxter [5]. In the BCSOS representation [6] a staggering of the vertex weights in the six-vertex models may be realized by covering the two interpenetrating simple cubic sublattices of a bcc lattice by two kinds of particles, each occupying all the sites of one of the two sublattices. A staggered field leaves the next-nearest-neighbor interactions on the two sublattices the same, but introduces different chemical potentials for the two types of particles. It becomes energetically more favorable for the crystal to have one type of particle in its topmost layer than the other type.

In this Letter, we find the phase diagram of the staggered F model and inverted F model (IF model), for which the coupling constant e is negative, by using the transfer-matrix technique and finite-size scaling. We show that the staggered field is relevant in the IF model for temperatures above a certain temperature T_R^I . Below this temperature, the staggered field is irrelevant. Thus, at temperatures below T_R^I an infinitesimal staggered field does not induce a transition to the ordered phase. However, a Kosterlitz-Thouless transition to the ordered state does occur at a temperature-dependent finite threshold value of the staggered field. In the BCSOS representation this corresponds to a crystal surface on which a facet appears for T above a staggered-field-dependent roughening temperature. When T approaches infinity this facet disappears again.

In order to find critical exponents and to examine the phase diagram we use a renormalization-group mapping of the BCSOS model onto the Gaussian model [10] and proceed in a way similar to that described in Ref. [11]. Since the amplitude of the height-height correlation function, $G(r) = \langle (h_r - h_0)^2 \rangle$, is kept invariant under renormalization, the amplitude of this correlation function of

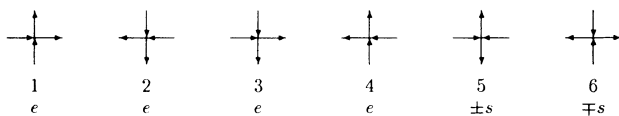


FIG. 1. The six possible vertices and their energies. The \pm and \mp signs refer to the two sublattices. For the F model e is positive, whereas e is negative in the IF model.

the BCSOS model in the rough phase can be identified with that of the Gaussian model [12]. For the $(I)F$ model without staggered field the asymptotic behavior of the former is given by [13]

$$G(r) \simeq \frac{2d^2}{\pi \arccos \Delta} \ln r \quad (T \geq T_R), \quad (1)$$

where d is the height difference between two nearest neighbors and Δ is equal to $1 - \frac{1}{2} \exp(2\beta e)$. For the Gaussian model on the other hand, one finds (see, e.g., Ref. [11] for details)

$$G(r) \simeq \frac{R}{2\pi^2} \ln r. \quad (2)$$

The parameter R denotes the Gaussian temperature. It is determined by requiring that the model renormalizes to the same fixed point as the BCSOS model. Thus we equate the amplitudes in the right-hand sides of Eqs. (1) and (2):

$$R = \frac{4\pi d^2}{\arccos[1 - \frac{1}{2} \exp(2\beta e)]} \quad (\beta e \leq \ln 2). \quad (3)$$

This result agrees with those obtained in Refs. [14–16], where the F model and the Gaussian model were related in a different way. We assume that the Gaussian and the BCSOS models indeed belong to the domain of attraction of the same fixed point, so that both models share the same set of critical exponents. In the Gaussian model, the exponents are associated with two classes of operators: the spin-wave operators and the vortex operators. They can be exactly calculated if the temperature R is known. Thus, the critical exponents for the BCSOS model can now be determined from those for the Gaussian model. In the first place we need the scaling dimensions [10] X_p^w of the spin-wave operators [11], which correspond to periodic potentials acting on the height variables,

$$X_p^w = \frac{R}{2p^2}, \quad (4)$$

where p is the period of the potential. The discreteness of the lattice corresponds to $p = d$. A staggered field corresponds to $p = 2d$, because subsequent layers energetically are not equivalent anymore, so the vertical period is increased to $2d$. The spin-wave operator is relevant if its dimension is smaller than 2, therefore the staggered field is relevant if $R < 16d^2$. From Eq. (3) we derive that $\beta e \gtrsim -0.2674$ (i.e., $k_B T_R^I \approx -e/0.2674$). This means that for all βe greater than this threshold value, even an arbitrarily small staggered field forces the system into an ordered state. A rough phase at nonzero values for the staggered field may only be found for negative values of the vertex energy e , i.e., in the IF model. According to renormalization-group arguments [12] such a rough phase will undergo a Kosterlitz-Thouless transition to the or-

dered state when the most relevant spin wave becomes marginal, i.e., $X_{2d}^w = 2$.

Other scaling dimensions of interest are those of the vortex operators [11],

$$X_q^s = \frac{q^2}{2R}, \quad (5)$$

associated with vortices of strength q . In the BCSOS model, a vortex-antivortex pair of this strength corresponds to a step of height q .

Thus, in zero staggered field the scaling dimensions follow from the Gaussian model. For nonzero staggered field, we use the transfer-matrix technique as described in Ref. [17]. This method yields the free energy and correlation lengths for $N \times \infty$ lattices. To obtain from these the scaling dimensions introduced above one has to apply finite-size scaling. According to the theory of phenomenological renormalization, a correlation length ξ_N of a finite system with linear lattice size N behaves at a critical point as $\xi_N \sim N$. A Kosterlitz-Thouless transition forms the boundary of a critical phase, so that one finds this behavior for a range of temperatures. Thus, if we plot N/ξ_N as a function of temperature for various system sizes, the graphs will converge as a function of system size for temperatures below the transition point. In conjunction to spin-wave and vortex operators one can define spin-wave and vortex correlation lengths, respectively, which can be obtained from the eigenvalues of the transfer matrix of the staggered IF model. This transfer matrix decomposes into $N + 1$ diagonal blocks, because each row of vertical arrows can only couple to another row that has an equal number of arrows pointing upwards (see, e.g., Ref. [5]). Both types of correlation lengths are connected to the eigenvalues of the transfer matrix by a relation of the form

$$\xi_N^{(k)} = \zeta / \ln \frac{\lambda_1}{\lambda_k}, \quad (6)$$

where λ_1 is the largest eigenvalue of the transfer matrix (located in the central block of the transfer matrix, with $N/2$ arrows pointing upwards) and the choice of the other eigenvalue λ_k is determined by the correlation function associated with $\xi_N^{(k)}$. For the correlation length associated with the $q = 2d$ vortex exponent (5), we set $\lambda_k = \lambda_2$, the largest eigenvalue of the subcentral block ($N/2 \pm 1$ arrows pointing upwards) of the transfer matrix. In the following, ξ_N will refer to this specific correlation length. The geometrical factor $\zeta = 2$ accounts for the fact that the transfer matrix adds two rows to the system at once. We have calculated and plotted N/ξ_N as a function of βs for several system sizes. For fixed $\beta e \gtrsim -0.2$ these graphs diverge for all $\beta s > 0$. However, for smaller (i.e., more negative) βe , there exists a range of (sufficiently small) βs where N/ξ_N displays convergent behavior as a function of N . This is shown in Fig. 2. These results are in agreement with our calculation for the threshold value

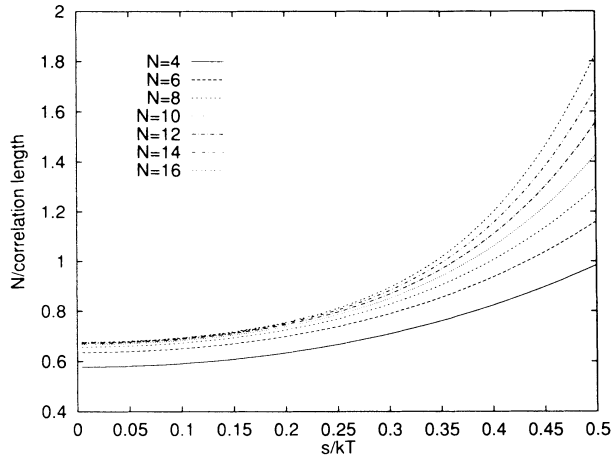


FIG. 2. The scaled inverse correlation lengths for $\beta e = -0.4$, as a function of βs .

of βe below which the staggered field is irrelevant and confirm our expectation that the staggered field induces a Kosterlitz-Thouless transition below T_R^I . It is difficult to find the precise location of this transition from the graphs. Therefore we use the prediction that X_{2d}^w becomes marginal. This implies that the amplitude of the height-height correlation function is constant all along the line of Kosterlitz-Thouless transitions [18–20]. So X_2^s is constant along this curve as well, being equal to $\frac{1}{8}$, the value it has for $\beta s = 0$ at $\beta e \approx -0.2674$. The requirement of covariance under conformal transformations leads to [21]

$$\lim_{N \rightarrow \infty} \frac{N}{\xi_N} = 2\pi X, \quad (7)$$

where X is the scaling dimension associated with the same correlation function as ξ_N , thus $X = X_2^s$. For a range of values for βs and $N = 4, \dots, 18$ the values of βe were calculated for which $N/\xi_N = \pi/4$. These values serve as finite-size estimates of the Kosterlitz-Thouless transition and were extrapolated to infinite systems using logarithmic and $1/N^2$ corrections [11]. Figure 3 shows the resulting phase diagram. The exactly solved $(I)F$ model corresponds to the vertical axis, where a phase transition occurs between two different ordered phases. For $e/k_B T > \ln 2$ this transition is discontinuous, whereas it is continuous for $-0.2674 \lesssim e/k_B T \leq \ln 2$. The curve indicates the Kosterlitz-Thouless transition induced by the staggered field. Its location is in good agreement with the points where the scaled inverse correlation lengths start to diverge (cf. Fig. 2). The area below the Kosterlitz-Thouless curve can be interpreted as a critical fan [22]. Note that for large $|s|$ this curve rapidly approaches $e = -|s| + \text{const}$. This is because for large $|s|$ vertices 1 through 4 compete with only one of the vertices 5 and 6 (depending on the sublattice); the remaining vertex is absent due to its high energy.

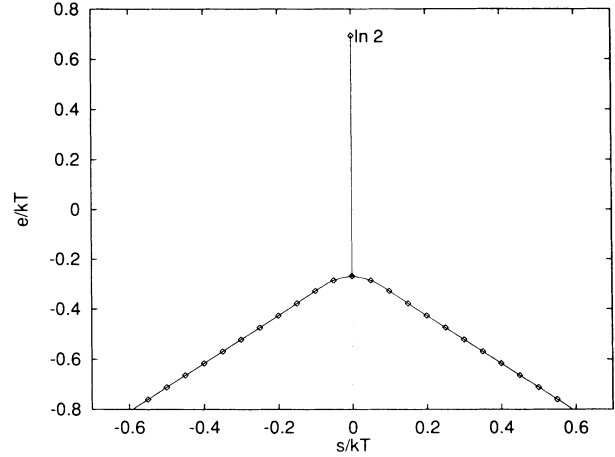


FIG. 3. The phase diagram of the F model and the IF model in a staggered field. The curve denotes the Kosterlitz-Thouless transitions. The area below this curve, including the curve itself, and the vertical axis up to $\beta e = \ln 2$ describe rough phases; the remaining area describes smooth ones.

From the phase diagram we can draw a remarkable conclusion. Suppose that the energy e is set to some negative value and the ratio e/s is fixed such that it has an absolute value greater than 1. Increasing the temperature from zero to infinity, we approach the origin of the phase diagram along a straight line which intersects the curve of phase transitions at some finite temperature T_{KT} . This means that we start in a rough (disordered) phase at $T = 0$ and enter a smooth (ordered) phase at T_{KT} . We propose calling this an inverse roughening transition, as in the BCSOS representation this transition corresponds to the appearance of a facet on a crystal surface at temperatures above T_{KT} . The diameter of this facet, relative to the system width, is proportional to the step free energy,

$$F_{\text{step}}(N) \sim \ln \frac{\lambda_1}{\lambda_2}, \quad (8)$$

where λ_1 and λ_2 have the same meaning as before. In Fig. 4 this quantity is plotted along the line $\beta e = -1.1\beta s$ for $0 \leq \beta s \leq 3.0$ for several values of N . Since this line is always in, or close to, a critical phase we use an iterated power-law extrapolation [11] for $N \rightarrow \infty$ (continuous line). The result is small in comparison with the finite-size results and therefore relatively inaccurate: the error at the maximum of the extrapolated curve is about 10%. From the correspondence between the step free energy as function of direct (i.e., nonstaggered) electric fields and the crystal form [23] it can be shown, using scaling arguments, that the step free energy (facet size) is proportional to $(\beta s)^{1/(2-X_{2d}^w)}$. Since $X_{2d}^w = \frac{3}{2}$ at the origin of the phase diagram, we see that the facet size is proportional to $(\beta s)^2$ for $T \rightarrow \infty$, in qualitative agreement with Fig. 4.

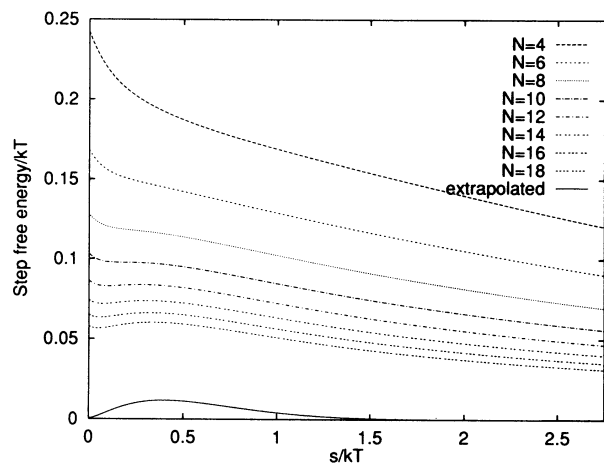


FIG. 4. The step free energy, which is proportional to the crystal facet size, as a function of βs , along the line $\beta e = -1.1\beta s$.

Inverse roughening is another example of entropically driven ordering [24]. At high enough temperatures the vertices 5 and 6 arrange themselves into a connected network with as many patches of vertices 1 through 4 as possible. The freedom of choosing the arrangement of horizontal and vertical arrows in each of these patches independently increases the entropy over that of configurations in which vertices 1 through 4 percolate. The entropy gain outweighs the energy cost of the vertices 5 and 6.

May inverse roughening transitions be expected for real crystals? For a binary crystal of the type described above [25] a realistic description will usually require not only a staggered field, but also a staggering of the weights of the vertices 1 through 4 [8,26,27]. However, also in that case the lattice period in the vertical direction is doubled, so for weak staggering one expects facet roughening to occur for $\beta e \lesssim -0.2674$, just as in the case studied here. Hence one should generally expect inverse roughening transitions in crystals with a staggered BCSOS structure, strong nearest-neighbor attraction and repulsion between next-nearest neighbors. Ionic crystals are obvious candidates for satisfying these requirements, for example, CsCl is known to have a structure of just the type we are looking for.

Finally we want to observe that in the BCSOS representation one can easily introduce fields with a vertical period larger than 2, which, e.g., could be realized physically for a period of 3 by making an $ABCABC\dots$ type stacking of layers. In this case the inverse roughening transition for weak staggering can be obtained again by

solving (3) for $R = 4p^2$ (with $p = 3, 4, \dots$), yielding a sequence of increasingly lower inverse roughening temperatures.

* Present address: Faculty of Applied Physics, Delft University of Technology, P.O. Box 5046, 2600 GA Delft, The Netherlands.

- [1] E. H. Lieb and F. Y. Wu, in *Phase Transitions and Critical Phenomena*, edited by C. Domb and M. S. Green (Academic Press, London, 1972), Vol. 1, pp. 331-490.
- [2] E. H. Lieb, *Phys. Rev. Lett.* **18**, 1046 (1967).
- [3] B. Sutherland, *Phys. Rev. Lett.* **19**, 103 (1967).
- [4] C. P. Yang, *Phys. Rev. Lett.* **19**, 586 (1967).
- [5] R. J. Baxter, *Exactly Solved Models in Statistical Mechanics* (Academic Press, London, 1982).
- [6] H. van Beijeren, *Phys. Rev. Lett.* **38**, 993 (1977).
- [7] F. Rys, *Helv. Phys. Acta* **36**, 537 (1963).
- [8] M. den Nijs, *J. Phys. A* **12**, 1857 (1979).
- [9] R. J. Baxter, *Phys. Rev. B* **1**, 2199 (1970).
- [10] B. Nienhuis, in *Phase Transitions and Critical Phenomena*, edited by C. Domb and J. L. Lebowitz (Academic Press, London, 1987), Vol. 11, pp. 1-53.
- [11] H. W. J. Blöte and M. P. Nightingale, *Phys. Rev. B* **47**, 15046 (1993).
- [12] B. Nienhuis, H. J. Hilhorst, and H. W. J. Blöte, *J. Phys. A* **17**, 3559 (1984).
- [13] R. W. Youngblood and J. D. Axe, *Phys. Rev. B* **21**, 5212 (1980).
- [14] L. P. Kadanoff and A. C. Brown, *Ann. Phys. (N.Y.)* **121**, 318 (1979).
- [15] H. J. F. Knops, *Ann. Phys. (N.Y.)* **128**, 448 (1980).
- [16] H. J. F. Knops, *Ann. Phys. (N.Y.)* **138**, 155 (1982).
- [17] Y. M. M. Knops, B. Nienhuis, H. J. F. Knops, and H. W. J. Blöte, *Phys. Rev. B* (to be published).
- [18] J. M. Kosterlitz and D. J. Thouless, *J. Phys. C* **6**, 1181 (1973).
- [19] J. M. Kosterlitz, *J. Phys. C* **7**, 1046 (1974).
- [20] D. R. Nelson and J. M. Kosterlitz, *Phys. Rev. Lett.* **39**, 1201 (1977).
- [21] J. L. Cardy, *J. Phys. A* **17**, L385 (1984).
- [22] M. Kohmoto, M. den Nijs, and L. P. Kadanoff, *Phys. Rev. B* **24**, 5229 (1981).
- [23] A. F. Andreev, *Zh. Eksp. Teor. Fiz.* **80**, 2042 (1981) [*Sov. Phys. JETP* **53**, 1063 (1982)].
- [24] M. Dijkstra and D. Frenkel, *Phys. Rev. Lett.* **72**, 298 (1994).
- [25] In fact one may rescale each of the lattice constants so as to obtain a body-centered rhombic (bcr) lattice (a special case of which is the fcc lattice) without changing the six-vertex representation of the model.
- [26] H. J. F. Knops, *Phys. Rev. B* **20**, 4670 (1979).
- [27] F. J. Wegner, *J. Phys. C* **5**, L131 (1972).